CHAPTER 4

HEATING CHARACTERISTICS OF THE PORTABLE HEATING SETUP

4.1 Introduction

This chapter describes the heating characteristics of the portable heating set up and the thermal conductivity measurement of 45S5 bioglass using the setup.

4.2 Determination of heating characteristics (first setup)

To perform an experiment at elevated temperature, the standard deviation of temperature on the sample surface must be less than 5%. Therefore, a thermal imaging camera has been used to determine the standard deviation of temperatures. The experiments have been performed in still air at room temperature. Room temperature will influence the convective heat transfer from the exposed surfaces of samples. There will be more heat transfer from the surfaces with lower room temperature. It will affect the time to attain a

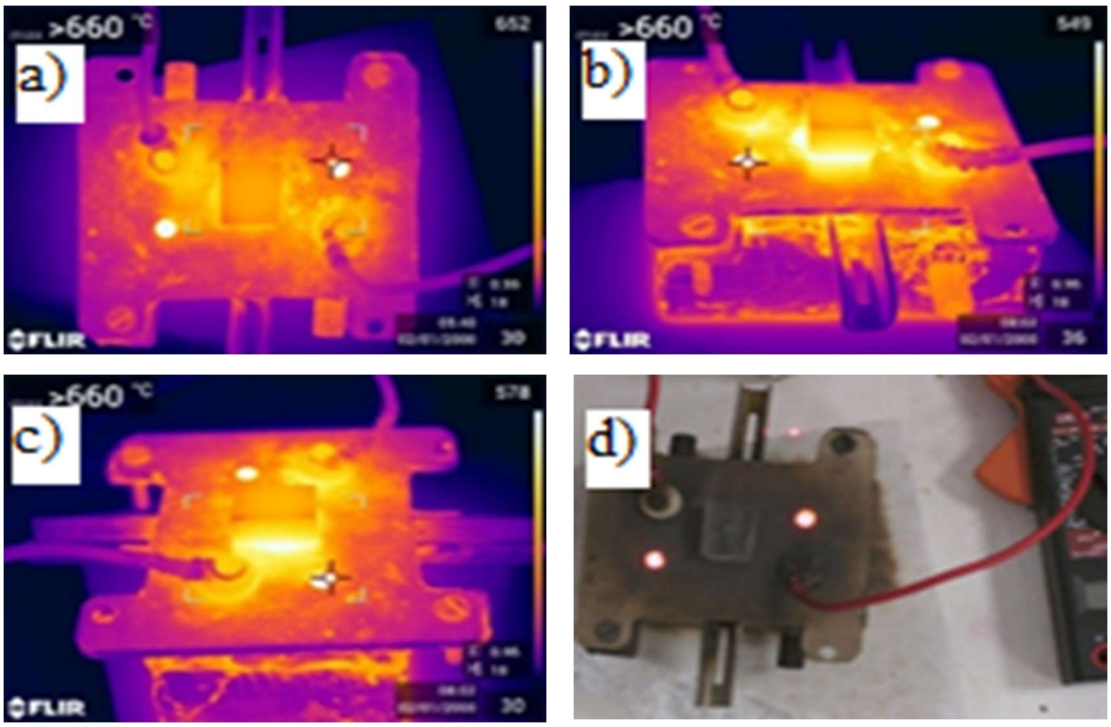

Figure 4.1:Thermal images; (a) top view, (b) along contact of length edge to the heat plate (L orientation), (c) along contact of width edge to the heat plate (B orientation) and (d) Normal camera image

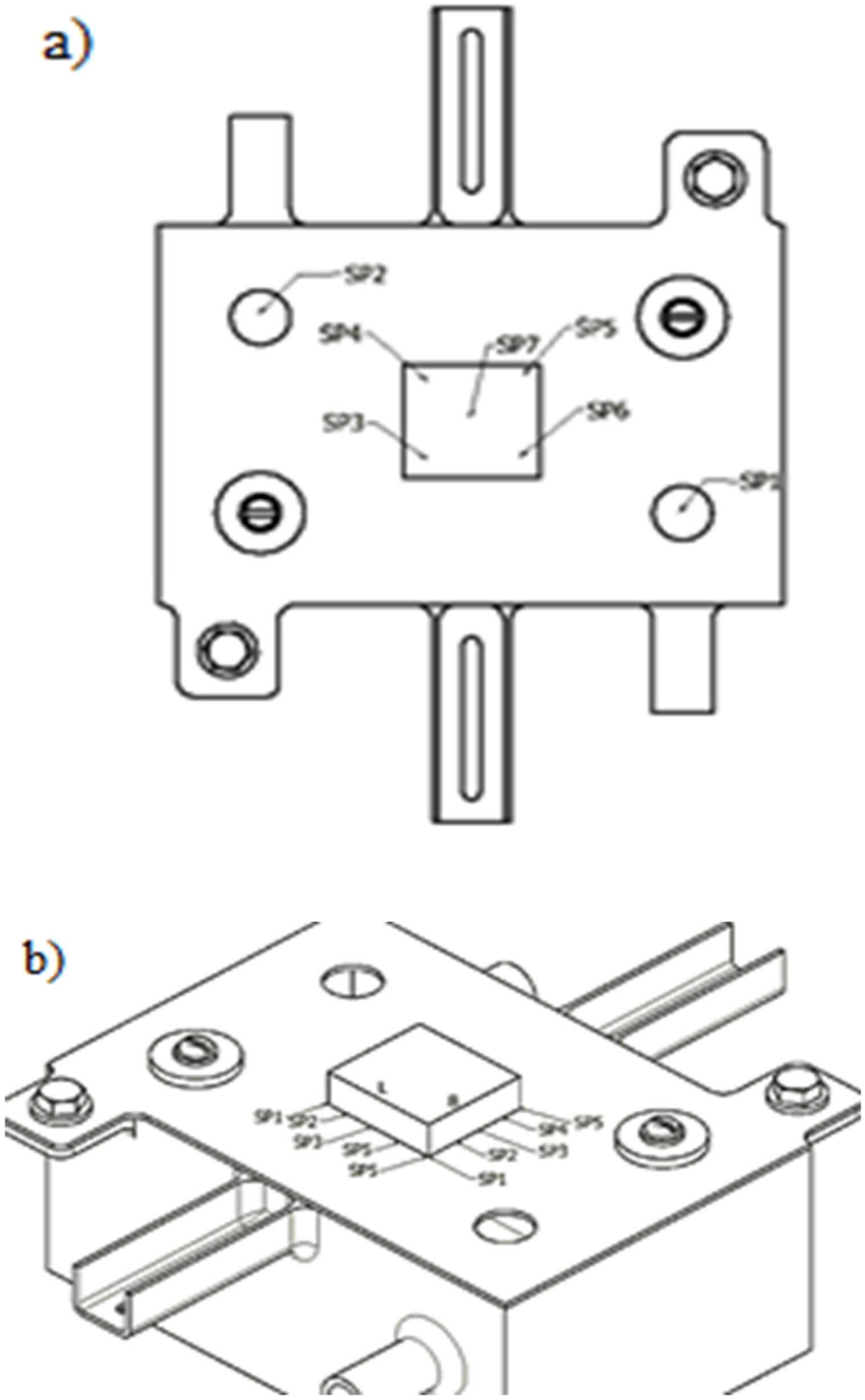

Figure 4.2: Temperature spot positions measured with infrared camera: (a) 'Top' orientation and (b) 'L & B' orientation

steady state. The room temperature was affected by the heating setup, but this variation

was 30.5 °C–31.5 °C for the experiment time duration of 35 min. Therefore, the average room temperature has been taken at 31 °C. The motive of the experimentation was to find the time required to reach a steady state at each current value and the corresponding suitable values of the sample surface temperature. After taking readings at each current value, the heater has been switched off to achieve an initial room temperature condition. The steady-state time has been recorded by keeping the IR camera in a continuous mode and waiting for the next 10 min with no further temperature rise from the last temperature value. No further rise in temperature shows that the heat generated by the heating coil is equal to the heat transferred to the environment. This satisfies the condition to achieve a steady state. The placements of IR camera has already been discussed in previous chapter (Chapter 3, section 3.4.3) as shown in Figure 3.16. Accordingly, Figure 4.1 shows all the different views of thermal images along with the original image samples. Figure 4.1(a) shows the thermal image top view, Figure 4.1(b) shows the thermal image along the contact of the long edge to the heat plate (L orientation), Figure 4.1(c) shows the thermal image along the contact of width edge to the heat plate (B orientation) and Figure 4.1(d) shows a normal camera image of top view taken from IR camera. Here, the top surface temperature of the sample and the heat plate temperature have been measured. Referring to Figure 4.2, the sample top surface temperature is measured from the top view IR image of the heater and the heat plate temperature is measured using IR images along L and B orientations. Five temperature spots have been selected and averaged in every thermal image in all three orientations; the top view as shown in Figure 4.2(a), the view along the contact of the long edge to the heat plate termed as ‘L’ orientation and the view along the contact of width edge to the heat plate termed as ‘B’ orientation as shown in Figure 4.2(b).

Table 4.1 shows all images taken at 1.5, 2.0, 2.5, 3.0, 3.5, 4.0 and 4.5 A. Steady state time for every sample has been recorded for every current value.

Table 4.1: Thermal images of set up along L, B and Top orientations at different currents with corresponding steady state time.

Current, I (A)	Steady Stae Time, Ts(Sec.)	L	B	Top
1.5	224	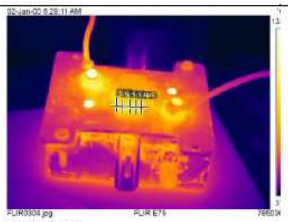	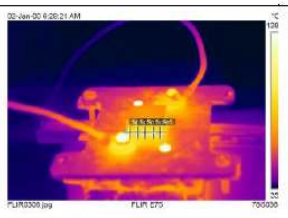	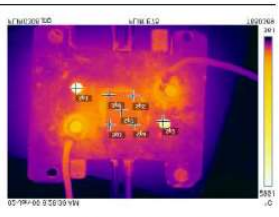
2.0	416			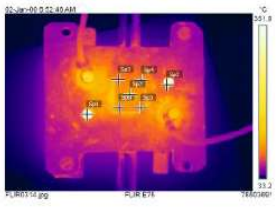
2.5	482		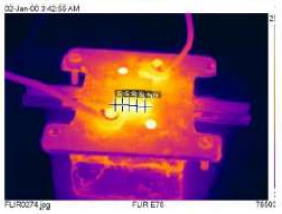	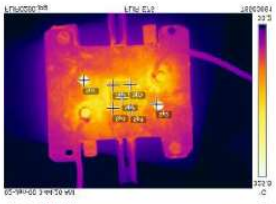
3.0	849	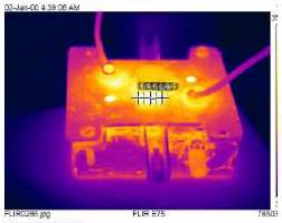	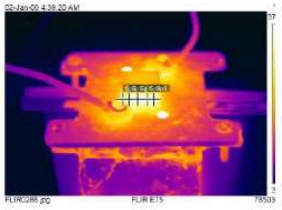	
3.5	1132	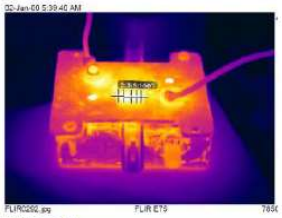	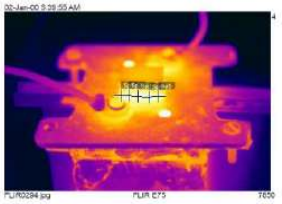	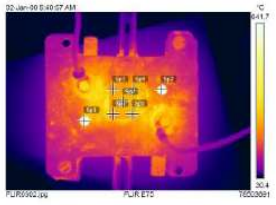
4.0	1631	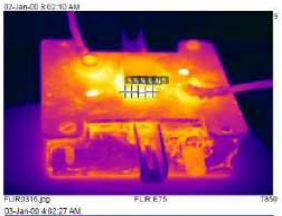	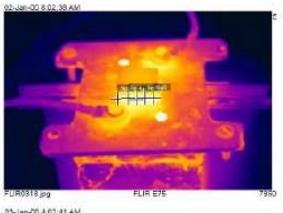	
4.5	1946	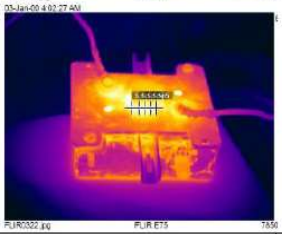		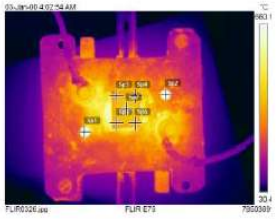

Table 4.2: Temperatures obtained along L, B and Top orientation

Orientations	Current, I (Amp.)	1.5	2	2.5	3	3.5	4	4.5
L	**SP1**	105.7	175.2	252.9	361.9	467.2	550.8	632.8
	SP2	105.6	174.8	257.4	371.7	460.2	562.3	605.2
	SP3	106.7	174.1	259	373.4	471.5	562.9	614.8
	SP4	106.3	169.7	257.1	359.9	469.1	548.9	605.2
	SP5	105.7	168.2	254.6	361.3	464.2	553.3	580.2
	L_{avg}	**106.0**	**172.4**	**256.2**	**365.6**	**466.4**	**555.6**	**607.6**
	SD	**0.5**	**3.2**	**2.4**	**6.4**	**4.4**	**6.5**	**19**
	%SD	**0.5**	**1.9**	**0.9**	**1.8**	**0.9**	**1.2**	**3.1**
B	**SP1**	104.1	175.3	241.2	357.9	448.2	525.6	601.2
	SP2	107.9	181.2	257.8	370.3	466.4	548.7	630.7
	SP3	109.4	185.2	258.4	382.5	482	581.3	651.4
	SP4	109.4	185.1	260.2	382.6	476.2	558	656.9
	SP5	107.1	179.8	256.8	374.7	463.3	553.2	643.6
	B_{avg}	**107.5**	**181.3**	**254.8**	**373.6**	**467.2**	**555.6**	**607.6**
	SD	**2.2**	**4.1**	**7.7**	**10.2**	**13**	**20**	**22.2**
	%SD	**2**	**2.3**	**3**	**2.7**	**2.8**	**3.6**	**3.5**
Top	**SP3**	76.6	113.8	178.3	247.6	310.3	363.6	415.1
	SP4	79.3	124.1	184.1	258.6	325.7	370.4	425.5
	SP5	81.1	129.3	191.1	261.5	327.1	377.1	428.6
	SP6	77.2	125.7	187.7	246.4	306	365.5	406.7
	SP7	85	137.7	203.6	282	351.1	404.5	457.4
	Top_{avg}	**79.8**	**126.1**	**188.9**	**259.2**	**324.0**	**376.2**	**426.6**
	SD	**3.4**	**8.7**	**9.5**	**14.4**	**17.7**	**16.6**	**19.2**
	%SD	**4.3**	**6.9**	**5**	**5.6**	**5.5**	**4.4**	**4.5**

After getting the thermal images at different temperature ranges, one needs to be sure that the standard deviation of temperature on the sample surface should be less than 5% to acquire appropriate data. Therefore, five spots, SP1, SP2, SP3, SP4 and SP5 have been taken at the sample top surface, along L and B as shown in Figure 4.2(a) and (b). The percentage standard deviation of temperature changes has been calculated at current 1.5, 2.0, 2.5, 3.0, 3.5, 4.0 and 4.5 A. The reports of all thermal images are shown in Annexure-II.

The percentage standard deviations (%SD) for top surface temperatures at different currents are shown in Table 4.2. The Maximum % SD of temperature for the top surface

is 6.9 % at 2.0 A. The % SD for the L side at different currents are shown in Table 4.2. The Maximum % SD of temperature for the L side is 3.1% at 4.5 A, which is an expected range. The values of % SD along 'B' at different currents are shown in Table 4.2. The Maximum % SD of temperature for B side is 3.6 % at 4.0 A. It has been observed with the help of % SD that the whole setup is performing quite well for temperatures up to 426.7 °C. Therefore, elevated temperature testing can be performed with appropriate accuracy because this setup has an acceptable range of temperature along Top, L and B orientations.

Table 4.3: Average heat plate temperatures (L+B)/2 and sample surface temperature $(Top)_{avg}$ with time - steady state (T_s) corresponding to current

I	L_{avg}	B_{avg}	$(L_{avg}+B_{avg})/2$	Top_{avg}	Ts (Sec.)
1.5	106.0	107.5	106.7	79.8	247
2	172.4	181.3	176.8	126.1	416
2.5	256.2	254.9	255.5	189.0	482
3	365.6	373.6	369.6	259.2	849
3.5	466.4	467.2	466.8	324.0	1132
4	555.6	553.4	554.5	376.2	1631
4.5	607.6	636.8	622.2	426.7	1946

Heating characteristic graphs are required to understand the heating behaviour of the setup for a particular sample. The average temperatures of the heat plate and top surface during the heating process have been considered for plotting these graphs. Since the temperatures of sides L and B have been measured with an IR camera, it has been assumed that the lower surface temperature of the sample is the average of both side L (L_{avg}) and side B (B_{avg}). Therefore, the average heat plate temperature $(L_{avg}+B_{avg})/2$ has been calculated in Table 4.3 and the average sample top surface temperature (Top_{avg}) has been taken from Table 4.2. The steady state time corresponding to the current value supplied to the heating coil is taken from Table 4.1. MiniTab 18 has been used for the regression analysis. The quadratic regression model is used to obtain function from the fitted curve for the current versus time-steady state. While the linear regression model is used to

obtain function from the fitted curve for current versus avg. heat plate temp and current versus sample surface temp. With the help of these operating graphs, it would be possible to find out the maximum temperature that can be achieved and steady state time at various

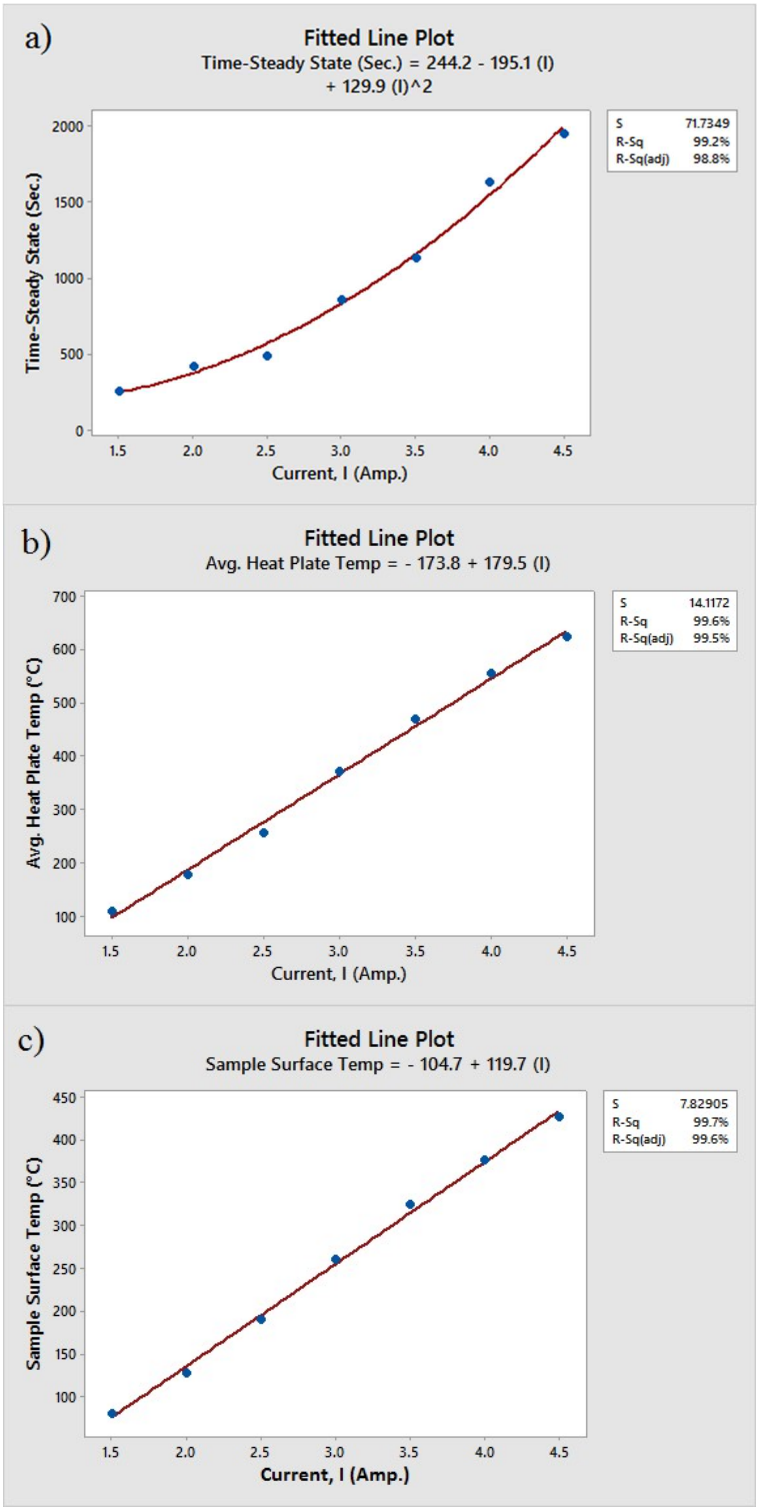

Figure 4.3: (a) Time-steady state (s) vs. current, I (A) (b) Avg. heat plate temperature (°C) vs. current, I (A), (c) Sample surface temperature (°C) vs. current, I (A)

currents. Figure 4.3(a) shows the graph, current, I (A) vs. time - steady state (Ts). The heat generated in the heater will be higher because the generated heat will be proportional to the product of the coil resistance and the square of the current supplied. So, the generated heat will be in a quadratic manner. Subsequently, the heat generated must be equal to the heat rejected from the heater to the surroundings to achieve a steady state. Since the higher heat will take relatively more time to escape to the surroundings and hence the required time to reach the steady state will also be more quadratically. Therefore, the obtained graph is found to be non-linear in nature. The steady-state time can be determined at every current value between 1.5 A - 4.5 A from the graph. Figure 4.3(b) shows the graph, current vs. average heat plate temperature, and average heat plate temperature as a function of the current. Current can be varied with the help of a heat controller and different average heat plate temperatures are obtained by varying the current following the graph shown in Figure 4.3(b). Figure 4.3(c) shows the surface temperature variation on the sample according to the current at the steady state of the system so that one can achieve temperature by setting the current value according to the graph. The approximate time taken to reach the required temperature can be seen from the graph plotted between current and steady-state time as shown in Figure 4.3(a).

4.3 Heating characteristics of the upgraded heating setup

The purpose of this setup is to provide convenience as well as portability so it could be installed on most of the machining and testing devices. Machining and testing at elevated temperatures can easily be performed with the help of this setup at a controlled temperature. The heat is generated through the joule's effect. The heating coil is made of nichrome wire. Its wire diameter is 2.0 mm and the coil diameter is 8 mm. The resistance of this coil is set at R = 2 Ω. The coil should have a maximum current capacity of 30 A.

The workpiece holder can hold 22 × 20 × 12 mm^3 of sample size. Heat flow through the heating coil is, $q_1 = I^2.R = (26^2).2 = 1352$ W (max).

This setup can be easily mounted on different machines like a scratch tester, vertical milling center (VMC), grinding heads, etc. to perform elevated temperature tests and operations just like the first setup. The upgraded setup is capable to heat the samples to 1000 ℃. The heat is controlled by a 220 V AC controller. A 45S5 bioglass sample has been heated for testing purposes. Figure 4.4 shows the heating chart corresponding to the current flow.

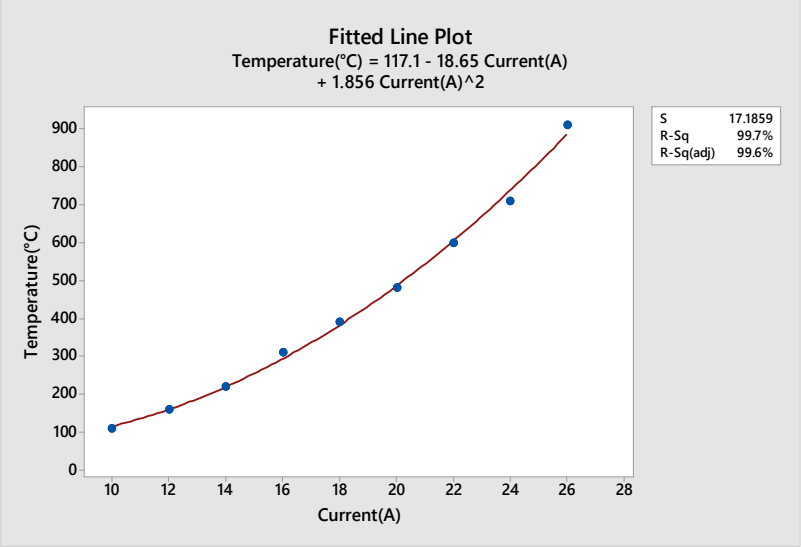

Figure 4.4: The heating chart corresponding to the current

4.4 Thermal conductivity measurement

This section is to explore the additional capability of the multipurpose portable heating setup although the measurement of the thermal conductivity is not going to contribute to the ductile regime machining. The thermal conductivity for glasses ranges from 1.38 W/m-K (for pure quartz glass) to roughly 0.5 W/m-K (for heavy lead content glasses) at ambient temperature. This value for the most widely used silicate glasses ranges from 0.9 to 1.2 W/m-K. In this research work, the thermal conductivity of 45S5 bioglass has been

derived using the portable heating setup. During initial experiments, there was three-dimensional mode of heat transfer. There is heat loss from all exposed surfaces of the sample during the heating. One surface that is in contact with the heat plate will absorb heat while the other 5 sides of the sample will reject the heat to the environment. Apparently, the thermal conductivity can be easily measured through the one-dimensional heat transfer. Therefore, it was needed to convert it to one-dimensional conductive heat transfer. Although, this is a fact that we cannot convert the system to a completely one-dimensional mode of heat transfer. Therefore, the side walls of the sample were covered with thermal insulation as shown in the setup represented in Figure 4.5. A ceramic fibre board (Make-Murugappa Morgan Thermal Ceramics Ltd., type-AZS) is used as insulation material having a thermal conductivity of 0.11 W/m-K at a mean temperature of 600 °C (ASTM C 201). The heat transferred through the insulating walls was neglected to acquire approximate one-dimensional heat transfer. A k-type thermo-couple was mounted in the heat plate on the contact edge of the sample such that the bottom surface temperature of the sample can be measured. The thermocouple was soldered to the heat plate to ensure intact contact. The upper surface temperature is measured with the help of an Infrared thermometer. The same sample of 45S5 bioglass has been taken

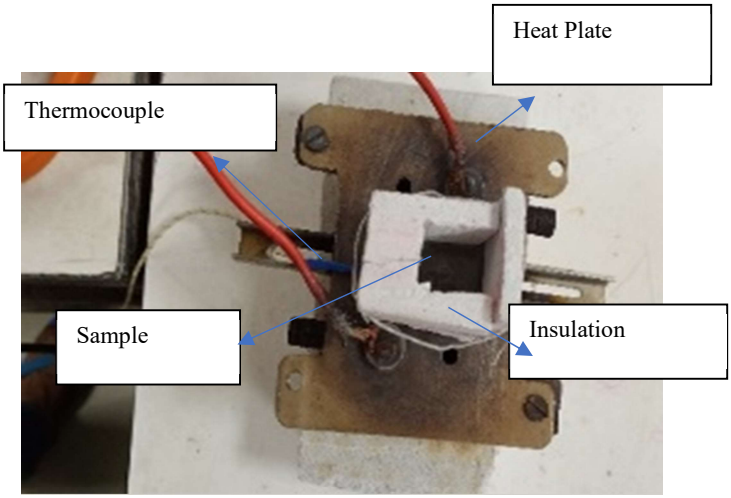

Figure 4.5: Setup for determining thermal conductivity

for the experiments. For a glass material surface, the emissivity of the infrared thermometer fluke 572-2 has been set to 0.95 and operated at a distance of 1 m.

Considering one-dimensional conductive heat flux in the system,

$$q = kA\frac{t_1 - t_2}{x} \tag{4.1}$$

where, k is thermal conductivity of sample, t_1 is heat plate temperature, t2 is sample top surface temperature, x =10 mm = 0.01 m i. e. sample height.

$$k = \frac{qx}{A(t_1 - t_2)} \tag{4.2}$$

From eqn (3.1) & (3.2)

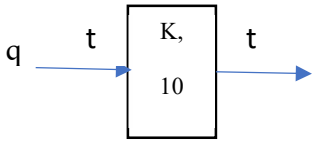

$q_1 = I^2.R$, and $q = \frac{A_2}{A_1} q_1 = 0.132 q_1$ (4.3)

Where, A_2 =contact area of the sample (Section 3.4.1, Equation 3.3) =425.5 mm^2

A1= projected area of the heater (Section 3.4.1, Equation 3.2) = 3212 mm^2

Table 4.4: Calculation of thermal conductivity of 45S5 bioglass

S. N.	Amp.	Heat Plate Temp, t_1(°C)	Sample Surface Temp, t_2(°C)	Resistance, R (Ω)	Projected Area Heater, A_1(mm^2)	q_1 (Heat total Area)	Contact Area, A_2 (mm^2)	q (Heat Sample Area)	Conductivity, K (W/m-K)
1	1.5	65	50	2.8	3212	6.3	425.5	0.83	1.3
2	2	204	170	2.8	3212	11.2	425.5	1.48	1.02
3	2.5	272	221	2.8	3212	17.5	425.5	2.32	1.07
4	3	392	322	2.8	3213	25.2	425.5	3.35	1.12
5	3.5	457	370	2.8	3212	34.3	425.5	4.54	1.23
6	4	509	394	2.8	3214	44.8	425.5	5.96	1.21
Average Thermal Conductivity of Bioglass Sample (K)									**1.16**

By putting all values in Table 4.4 the value of conductivity is calculated for 45S5 bioglass. The values of thermal conductivity of 45S5 bioglass are found between 1.30 W/m-K and 1.02 W/m-K with an average of 1.16 W/m-K between temperatures 50 °C to 509 °C. Any material's thermal conductivity is influenced by both molecular vibrations and free electron motion. The movement of free electrons is primarily responsible for the thermal conductivity of metals. The molecular vibrations increase with increasing temperature. Therefore, they hinder the free electron movement, which lowers conductivity. There are no free electrons in the case of non-metals. Thus, heat conduction is only caused by molecular vibrations, and for non-metals, conductivity rises as temperature rises. This is why, table 4.4 illustrates that the conductivity of the bioglass is increasing from 204 °C to 457 °C. The conductivity for experiments no. 5 and 6 is approximately the same. The conductivity for experiment no. 1 is more than the rest of the values. Experimental error is the possible reason for these variations.

4.5 Summary

A portable heating setup of overall dimensions 105 x 150 x 53 mm^3, has been successfully designed and fabricated. This can be used for heating the samples in multiple applications such as scratch testing, indentation testing, machining on VMC of ceramic samples and grinding. Different average temperatures on the sample surface and heat plate can be achieved with the help of the given graphs in Figures 4.3 and 4.4 along with their time taken to reach a steady state with an appropriate temperature distribution on the surface. The maximum standard deviation of temperature on the working area of the sample top surface, along L and B is 5.6%, 3.6% and 3.1%, which is an appropriate range to perform experiments. With the use of this setup, the average value of thermal conductivity of 45S5 bioglass is found to be 1.16 W/m-K. This setup is having great utility in the machining

and testing of hard and brittle materials, due to its portability, easy operation and capability to soften the material by preheating them.